

Primordial power spectra for curved inflating universes

Will Handley ^{*}

*Astrophysics Group, Cavendish Laboratory, J.J.Thomson Avenue,
Cambridge, CB3 0HE, United Kingdom;*

*Kavli Institute for Cosmology, Madingley Road, Cambridge, CB3 0HA, United Kingdom;
and Gonville and Caius College, Trinity Street, Cambridge, CB2 1TA, United Kingdom[†]*



(Received 22 July 2019; published 12 December 2019)

Exact numerical primordial power spectra are computed and plotted for the best-fit *Planck* 2018 curved universe parameters. It is found that the spectra have generic cutoffs and oscillations within the observable window for the level of curvature allowed by current cosmic microwave background measurements and provide a better fit to current data. Derivations for the Mukhanov-Sasaki equation for curved universes are presented and analyzed, and theoretical implications for the quantum and classical initial conditions for inflation are discussed within the curved regime.

DOI: [10.1103/PhysRevD.100.123517](https://doi.org/10.1103/PhysRevD.100.123517)

I. INTRODUCTION

Cosmological inflation [1–3] is the current most popular theory for explaining the observed flatness and homogeneity of our present-day universe, while simultaneously providing a powerful framework for predicting the measured spectrum of anisotropies in the cosmic microwave background [4,5]. Nevertheless, small and unsatisfactory features in the cosmic microwave background (CMB) power spectra arguably still remain [6], and there are ever-increasing tensions observed between datasets that measure the early universe and those that measure late-time properties [7–12]. The hunt is on to find extensions to the concordance cosmology (cosmological constant with cold dark matter— Λ CDM) which are capable of resolving some or all of these discrepancies.

One extension that is often considered is to reintroduce a small amount of late-time curvature, creating a $K\Lambda$ CDM cosmology [13,14]. *Planck* 2018 data without the lensing likelihood [15] give relatively strong evidence for a closed universe [4]. Adding in lensing and Baryon acoustic oscillation data [16–18] reduces this evidence considerably, but it remains an open question as to why the CMB alone strongly prefers universes with positive spatial curvature (with possible implications for tension resolution). Nevertheless, at the time of writing, universe models with percent-level spatial curvature remain compatible with current datasets.

There are theoretical reasons to consider the effect of curvature on the dynamics of inflation. If one is to invoke an inflationary phase in order to explain the observed

present-day flatness, one cannot assume that the universe was flat at the start of inflation, and the presence of any curvature is arguably incompatible with eternal inflation. Furthermore, the observation of any amount of present-day curvature strongly constrains the total amount of inflation, providing a powerful justification for just-enough-inflation theories [19–24].

In the traditional curved $K\Lambda$ CDM cosmology, a simple (A_s, n_s) parametric form for the primordial power spectrum is usually assumed [4,5],

$$\mathcal{P}_{\mathcal{R}}^{K\Lambda\text{CDM}}(k) = A_s \left(\frac{k}{k_*} \right)^{n_s - 1}. \quad (1)$$

In this work, I examine the effect on the fit of curved cosmologies to data if an exact numerical approach is used to calculate the primordial power spectrum. In all cases, an improved fit is found.

In Sec. II, the Mukhanov-Sasaki equation is derived in the general case of curved universes and compared with the flat-space equivalent. In Sec. III, the general Mukhanov action is calculated and discussed with regards to its quantization and consequent setting of initial conditions. In Sec. IV, the primordial and CMB power spectra are calculated for the best-fit *Planck* 2018 parameter values, and the fit is compared against the concordance case. Conclusions are presented in Sec. V.

II. THE MUKHANOV-SASAKI EQUATION

In this section for completeness, I derive the Mukhanov-Sasaki equation [Eq. (12)] for curved universes by a direct perturbative approach [25]. Similar computations have been performed historically by [26–32]. The analytical calculations throughout this paper were per-

^{*}wh260@mrao.cam.ac.uk

[†]<https://www.kicc.cam.ac.uk/directory/wh260>

med with the aid of computer algebra provided by Maple™ 2017 [33,34], making use of the PHYSICS and DIFFERENTIALGEOMETRY packages.

The action for a single-component scalar field minimally coupled to a curved spacetime is

$$S = \int d^4x \sqrt{|g|} \left\{ \frac{1}{2} R + \frac{1}{2} \nabla^\mu \phi \nabla_\mu \phi - V(\phi) \right\}. \quad (2)$$

Extremizing this action yields the Einstein field equations and a conserved stress energy tensor. Throughout this paper, in accordance with the cosmological principle, we shall assume that to zeroth order the solutions to these equations are homogeneous and isotropic. We then perturbatively expand these equations about the homogeneous solutions to first order in the Newtonian gauge, with the perturbation to the scalar field written as $\delta\phi$. In spherical polar coordinates, the metric is therefore

$$ds^2 = (1 + 2\Phi)dt^2 - a(t)^2(1 - 2\Psi)(c_{ij} + h_{ij})dx^i dx^j, \\ c_{ij} dx^i dx^j = \frac{dr^2}{1 - Kr^2} + r^2(d\theta^2 + \sin^2\theta d\phi^2), \quad (3)$$

where K denotes the sign of the spatial curvature, taking values of $K = +1$ for a closed (positively curved) universe, $K = -1$ for an open (negatively curved) universe, and $K = 0$ for a traditional flat universe. The covariant spatial derivative associated with the metric on comoving spatial slices is denoted with a Latin index as ∇_i with no factors of $a(t)$. The potentials Φ and Ψ along with $\delta\phi$ are scalar perturbations, while h_{ij} is a divergenceless, traceless tensor perturbation with two independent polarization degrees of freedom (d.o.f.).

A. Zeroth order equations

At zeroth order, the time-time component of the Einstein field equations and the time component of the conservation of the stress-energy tensor give the evolution equations of the homogeneous background fields

$$H^2 = \frac{1}{3} \left(\frac{1}{2} \dot{\phi}^2 + V(\phi) \right) - \frac{K}{a^2}, \quad (4)$$

$$0 = \ddot{\phi} + 3H\dot{\phi} + V'(\phi), \quad (5)$$

where the Hubble parameter $H = \dot{a}/a$, and primes denote derivatives with respect to ϕ . A further useful relation is

$$\dot{H} = -\frac{1}{2} \dot{\phi}^2 + \frac{K}{a^2}, \quad (6)$$

which may be found by differentiating Eq. (4) and eliminating the potential with Eq. (5). Equations (4) and (5) may be used to remove all explicit potential dependency from the first order equations, and Eq. (6) can be used to

remove all derivatives of H in place of ϕ , which is performed without comment in all of the below.

B. First order equations

To first order, the time-time component of the Einstein field equations gives

$$6H\dot{\Psi} + 2V\Phi + V'\delta\phi + \dot{\phi}\delta\dot{\phi} - \frac{2}{a^2} \nabla_i \nabla^i \Psi \\ - 6\frac{K}{a^2} (\Phi + \Psi) = 0. \quad (7)$$

The time-space components of the Einstein field equations all yield

$$\dot{\phi}\delta\phi - 2H\Phi - 2\dot{\Psi} = 0. \quad (8)$$

The time component of the conservation equation shows

$$2V'\Phi + V''\delta\phi - 3\dot{\phi}\dot{\Psi} - \dot{\phi}\dot{\Phi} - \frac{1}{a^2} \nabla_i \nabla^i \delta\phi + \delta\ddot{\phi} + 3H\delta\dot{\phi} = 0. \quad (9)$$

The off-diagonal spatial components prove that

$$\Phi = \Psi, \quad (10)$$

and the gauge-invariant comoving curvature perturbation is defined by the expression

$$\mathcal{R} = \Psi + \frac{H}{\dot{\phi}} \delta\phi. \quad (11)$$

Using the time derivative of (8), alongside Eqs. (7)–(9) we have four master equations. Substituting \mathcal{R} for Φ and Ψ into these using Eqs. (10) and (11) allows us to eliminate $\delta\phi$ and its first and second time derivatives, yielding the Mukhanov-Sasaki equation

$$0 = (\mathcal{D}^2 - K\mathcal{E})\dot{\mathcal{R}} + \left(\left(H + 2\frac{\dot{z}}{z} \right) \mathcal{D}^2 - 3KH\mathcal{E} \right) \dot{\mathcal{R}} \\ + \frac{1}{a^2} \left(K \left(1 + \mathcal{E} - \frac{2\dot{z}}{H z} \right) \mathcal{D}^2 + K^2\mathcal{E} - \mathcal{D}^4 \right) \mathcal{R}, \quad (12)$$

where

$$\mathcal{D}^2 = \nabla_i \nabla^i + 3K, \quad z = \frac{a\dot{\phi}}{H}, \quad \mathcal{E} = \frac{\dot{\phi}^2}{2H^2}. \quad (13)$$

Upon Fourier decomposition, one simply replaces the \mathcal{D}^2 operator in Eq. (12) with its associated scalar wave vector expression [35]

$$\begin{aligned} \mathcal{D}^2 &\leftrightarrow -k^2 + 3K, & k \in \mathbb{R}, k > 0: & \quad K = 0, -1, \\ \mathcal{D}^2 &\leftrightarrow -k(k+2) + 3K, & k \in \mathbb{Z}, k > 2: & \quad K = +1. \end{aligned} \quad (14)$$

One may interpret the operator \mathcal{D}^2 physically by examining the Ricci three scalar to first order

$$R^{(3)} = 6 \frac{K}{a^2} + \frac{4}{a^2} (c^{ij} \nabla_i \nabla_j + 3K) \mathcal{R}, \quad (15)$$

so the perturbation to comoving spatial curvature can be seen by inspection to be $\frac{4}{a^2} \mathcal{D}^2 \mathcal{R}$.

The Mukhanov-Sasaki equation (12) in the curved case demands some comment. First, it should be noted that for the flat case $K = 0$ it collapses down to its usual form, albeit with an additional $\nabla_i \nabla^i$ multiplying each term. The same observations apply for the small-scale limit $k \rightarrow \infty$. The addition of curvature considerably increases the complexity of the evolution equations at low and intermediate k by adding wave vector-dependent coefficients to all three terms in front of $\dot{\mathcal{R}}$, $\dot{\mathcal{R}}$, and \mathcal{R} . As we shall see in Sec. IV, this has consequences for the evolution of the comoving curvature perturbation and the resulting primordial power spectrum.

The tensor equivalent to Eq. (12) is derived similarly, yielding

$$\ddot{h} + 3H\dot{h} - \frac{1}{a^2} (\nabla_i \nabla^i - 2K) h = 0, \quad (16)$$

for both polarization modes of the tensor perturbation. Here the modification provided by curvature is significantly simpler, and readers can confirm that it reduces to the flat-space equivalent in the case that $K = 0$ and for $k \gg 1$.

III. THE MUKHANOV ACTION

In this section, I confirm the calculation in Sec. II by arriving at Eq. (12) via the Mukhanov action. I follow the notation of Baumann [36] (Appendix B), generalizing their calculation to the curved case.

The simplest approach for deriving the perturbation to the action in Eq. (2) is to write the metric in the ADM formalism [37,38], where spacetime is sliced into three-dimensional hypersurfaces

$$ds^2 = -N^2 dt^2 + g_{ij}^{(3)} (dx^i + N^i dt)(dx^j + N^j dt). \quad (17)$$

With the metric in this form, we find that the action from Eq. (2) becomes

$$\begin{aligned} S = \frac{1}{2} \int d^4x \sqrt{|g^{(3)}|} [NR^{(3)} + N^{-1} (E_{ij} E^{ij} - E^2) \\ + N^{-1} (\dot{\phi} - N^i \nabla_i \phi)^2 - N \nabla_i \phi \nabla^i \phi - 2NV], \end{aligned} \quad (18)$$

$$E_{ij} = \frac{1}{2} (\dot{g}_{ij}^{(3)} - \nabla_i N_j - \nabla_j N_i), \quad E = E_i^i. \quad (19)$$

Focussing on first order scalar perturbations, we write

$$N = 1 + \alpha, \quad N_i = \nabla_i \psi. \quad (20)$$

Working in the comoving gauge where $\delta\phi = 0$, the spatial part of the ADM metric is defined to be

$$g_{ij}^{(3)} = a^2 (1 - 2\mathcal{R}) c_{ij}. \quad (21)$$

The Lagrangian constraint equations are

$$\alpha = -\frac{\dot{\mathcal{R}}}{H} + \frac{K}{a^2} \frac{\psi}{H}, \quad (22)$$

$$\frac{1}{a^2 H} \mathcal{D}^2 \mathcal{R} - \mathcal{E} \dot{\mathcal{R}} = \frac{1}{a^2} \mathcal{D}^2 \psi - \frac{K}{a^2} \mathcal{E} \psi. \quad (23)$$

We may formally solve Eq. (23) explicitly for ψ with the rather cryptic expression

$$\psi = \frac{\mathcal{R}}{H} - a^2 \mathcal{E} (\mathcal{D}^2 - K\mathcal{E})^{-1} \left(\dot{\mathcal{R}} - \frac{K}{a^2} \frac{\mathcal{R}}{H} \right). \quad (24)$$

By the construction of the ADM formalism, substituting the first order solutions from Eqs. (22) and (23) into the action from Eq. (18) gives the second order action. After some effort integrating this by parts, we find

$$\begin{aligned} S = \frac{1}{2} \int d^4x \sqrt{|c|} a^3 \frac{\dot{\phi}^2}{H^2} \left\{ \left(\dot{\mathcal{R}} - \frac{K}{a^2} \frac{\mathcal{R}}{H} \right)^2 \right. \\ \left. - \frac{K}{a^2} \left(\dot{\mathcal{R}} - \frac{K}{a^2} \frac{\mathcal{R}}{H} \right) \left(\psi - \frac{\mathcal{R}}{H} \right) \right. \\ \left. - \frac{1}{a^2} \nabla_i \mathcal{R} \nabla^i \mathcal{R} + 3 \frac{K}{a^2} \mathcal{R}^2 \right\}. \end{aligned} \quad (25)$$

Substituting Eq. (24) into the above, and integrating by parts one more time returns the unusual action

$$\begin{aligned} \frac{1}{2} \int d^4x \sqrt{|c|} a^3 \frac{\dot{\phi}^2}{H^2} \left\{ \frac{1}{a^2} \mathcal{R} \mathcal{D}^2 \mathcal{R} \right. \\ \left. + \left(\dot{\mathcal{R}} - \frac{K}{a^2} \frac{\mathcal{R}}{H} \right) \frac{\mathcal{D}^2}{\mathcal{D}^2 - K\mathcal{E}} \left(\dot{\mathcal{R}} - \frac{K}{a^2} \frac{\mathcal{R}}{H} \right) \right\}. \end{aligned} \quad (26)$$

Varying this action with respect to \mathcal{R} recovers the Mukhanov-Sasaki equation from Eq. (12).

The full curved action is worthy of comment. Setting $K = 0$ recovers the flat-space action, but with nonzero K the action becomes nonlocal due to the presence of a denominator with a derivative term.

In the flat case, the usual next step is to diagonalize the action so that it has a canonical normalization¹ by transforming to conformal time $d\eta = a dt$ and rephrasing in

¹A canonically normalized quantum field ϕ with mass m has action of the form $S = \int dt d^3x \dot{\phi}^2 + \phi(-\nabla^2 + m^2)\phi$.

terms of the Mukhanov variable $v = z\mathcal{R}$. In the curved case, this is impossible. The best one can do is to define a wave vector-dependent \mathcal{Z} and v via

$$v = \mathcal{Z}\mathcal{R}, \quad \mathcal{Z} = \frac{a\dot{\phi}}{H} \sqrt{\frac{\mathcal{D}^2}{\mathcal{D}^2 - K\mathcal{E}}}, \quad (27)$$

in which case, the action becomes

$$\frac{1}{2} \int d\eta d^3x \sqrt{|c|} \left(v'^2 - (\nabla v)^2 + \left(\frac{\mathcal{Z}''}{\mathcal{Z}} + 2K + \frac{2K\mathcal{Z}'}{\mathcal{H}\mathcal{Z}} \right) v^2 \right). \quad (28)$$

The lack of canonical normalization implied by the k -dependent \mathcal{Z} has theoretical consequences for the initial conditions for inflation, since for low to intermediate k one cannot draw an analogy to the de Sitter case in order to define initial conditions. The correct theoretical choice for initial conditions in this case is far from clear, and it may be that the only way to differentiate between competing approaches is to choose the correct initial conditions via confrontation with data.

The tensor part of the action is

$$\frac{1}{16} \int d^4x \sqrt{|c|} a^3 \left(\dot{h}_{ij} \dot{h}^{ij} + \frac{1}{a^2} h_{ij} (\nabla_k \nabla^k - 2K) h_{ij} \right), \quad (29)$$

which even in the presence of curvature remains canonically quantizable in the traditional sense by switching to conformal time and making the variable redefinition $v_t = ah$.

IV. THE PRIMORDIAL POWER SPECTRUM

To compute the exact primordial power spectrum, the Mukhanov variable \mathcal{R} is evolved via the Mukhanov-Sasaki equation (12) for a relevant range of wave vectors k . The primordial power spectrum is then given by the limiting value of \mathcal{R} after horizon exit,

$$\mathcal{P}_{\mathcal{R}}(k) = \lim_{k \ll aH} \frac{k^3}{2\pi^2} |\mathcal{R}|^2. \quad (30)$$

The initial conditions for the evolution of the Mukhanov variable represent the injection of quantum mechanics into this system. For simplicity, I consider two types of initial conditions: Bunch-Davies (BD) and renormalized stress-energy tensor (RST), which are set at inflation start t_i ,

$$\mathcal{R}_i = \frac{1}{\sqrt{2kz_i}}, \quad \dot{\mathcal{R}}_i = \begin{cases} -i\frac{k}{a_i} - \frac{\dot{z}_i}{z_i} & \text{BD} \\ -i\frac{k}{a_i} & \text{RST.} \end{cases} \quad (31)$$

BD initial conditions are theoretically only appropriate for a de Sitter-like spacetime, which at inflation start for low- k

modes is not true, while RST initial conditions are designed to be valid in all regimes [39].

The numerical integration itself is most efficiently performed using a solver that is capable of accurately navigating the many oscillations between initial conditions and horizon exit. Such solvers have undergone recent development [40–43], and in this work I use the latest of these provided by Agocs *et al.* [42].

For the evolution of the background variables, I assume a *Planck* 2018 TTTEEE + lowl + lowE + lensing best-fit concordance $K\Lambda$ CDM curved cosmology, a monomial inflaton potential $V(\phi) \propto \phi^{4/3}$ and a reheating phase modeled by continuing the inflaton evolution until intersection with late-time Friedmann horizon. Interestingly, under this background setup, chaotic and Starobinsky potentials are incompatible with the *Planck* best-fit cosmology when curvature is included. The full pipeline of how these background evolutions are constructed will be discussed in an upcoming paper [44]. The $K\Lambda$ CDM parameters pin down all but 1 d.o.f. in the background evolution, leaving a single primordial parameter determining the degree of primordial curvature at the start of inflation, or equivalently the scale factor of the universe at inflation start a_i . For the curved case, the size of the universe at the start of inflation is bounded from below by the requirement that $H_i > 0$ and bounded from above by the requirement that the horizon problem is solved, i.e., that the amount of conformal time before inflation is greater than the amount of time afterward. This amounts to a constraint that $22k\ell_p < a_i < 171k\ell_p$. Beyond the lower bound the primordial curvature diverges as $H \rightarrow 0$ and the universe begins in an emergent coasting state [45,46]. Solutions for this case however are incompatible with the *Planck* best-fit parameters. The minimum amount of primordial curvature at the upper bound is -2.1% , the maximum amount of curvature is ~ -150 , and the “medium” amount of curvature in the figures is the geometric mean of these two.

The primordial power spectrum for the BD case is plotted in Fig. 1 and for RST initial conditions in Fig. 2. Relative to the concordance $K\Lambda$ CDM, which assumes the almost flat power spectrum from Eq. (1), including the exact numerical calculation introduces oscillations and a suppression of power at low k , independent of initial conditions. Varying the remaining d.o.f. provided by the amount of primordial curvature alters the oscillations and level of suppression in a nonmonotonic manner.

In both Figs. 1 and 2, these predictions for the primordial power spectrum are followed through to the CMB [47]. For all allowed values of initial primordial curvature, incorporating the exact numerical solution results in an improved $\Delta\chi^2$ relative to $K\Lambda$ CDM. Furthermore, the data are capable of distinguishing a preferred vacuum state, with the best fit preferring RST initial conditions over the traditional Bunch-Davies vacuum.

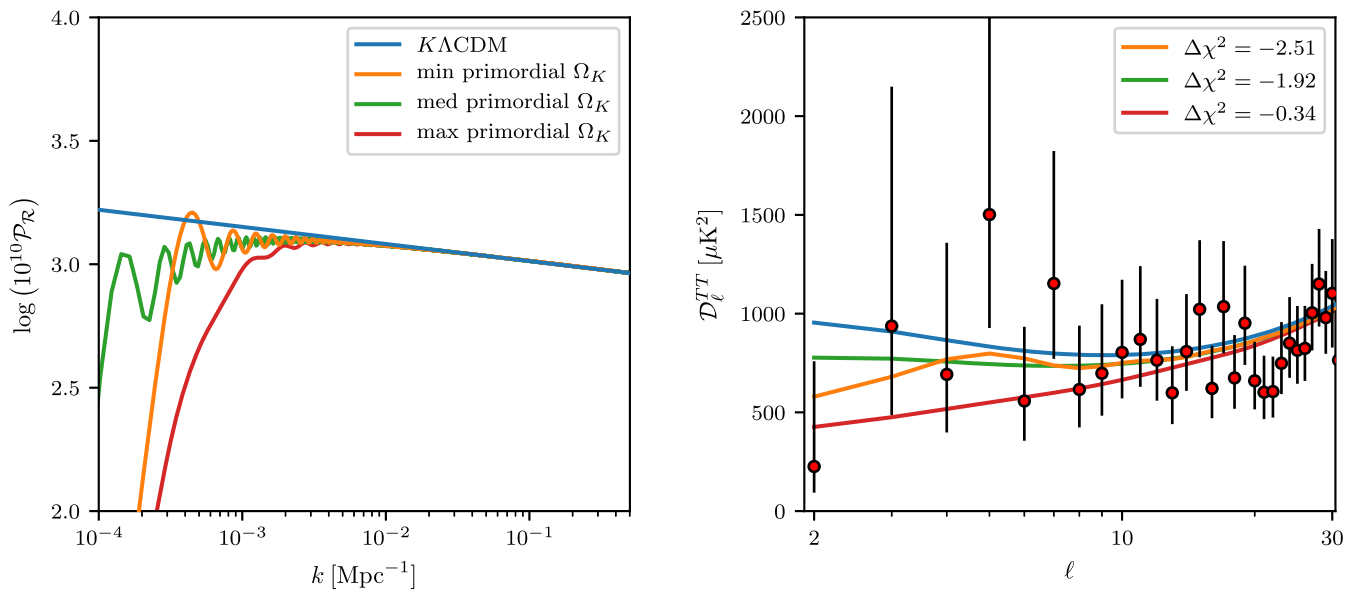


FIG. 1. Left: representative best-fit primordial power spectra corresponding to the range of allowed primordial curvatures. Oscillations and a generic suppression of power are visible at low k . The jagged edges of the curves at low k arise from the discreteness of the wave vectors for closed universes indicated in Eq. (14). Right: the corresponding low- ℓ effects on the CMB power spectrum. The improvement in $\Delta\chi^2$ relative to $K\Lambda$ CDM is shown in the right-hand figure legend, with negative values indicating a better fit to the data. The best-fit spectra without including the full primordial power spectrum calculation is highlighted in blue. Plots are shown for the entire observational window for Planck-like data on the left, and the plot on the right highlights the deviating region for the CMB power spectrum. There is no appreciable deviation from the traditional power spectrum at higher k and ℓ values.

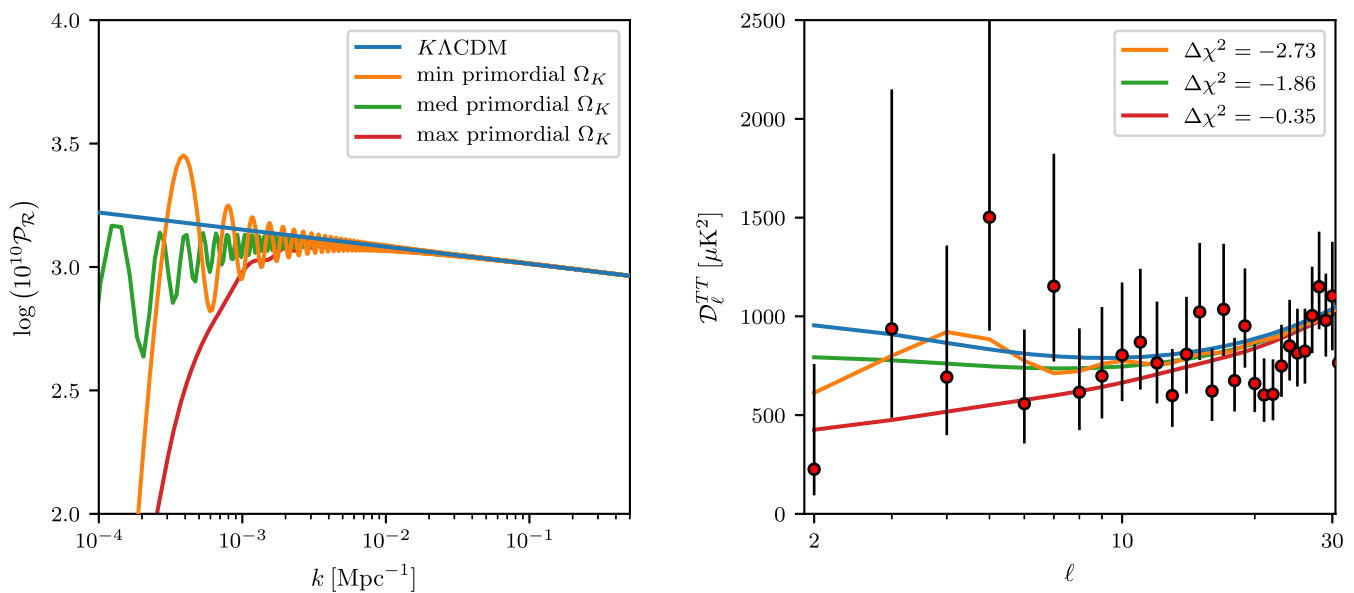


FIG. 2. Same as Fig. 1, but using RST initial conditions instead of BD from Eq. (31). The oscillations in the primordial power spectrum (left panel) are enhanced by RST initial conditions, resulting in a change in the $\Delta\chi^2$ for all cases, and a marginally better fit for the best-fitting case (right panel).

It should be noted that these $\Delta\chi^2$ values are not derived from a true fitting procedure. First, in the absence of a publicly available likelihood at the time of writing, the approximate $\Delta\chi^2$ value is computed from the available

compressed C_ℓ spectra and their error bars. Second (for similar reasons), I have used the best-fit cosmological parameters derived from the $K\Lambda$ CDM data with the default spectrum, rather than a full fit with the modified power

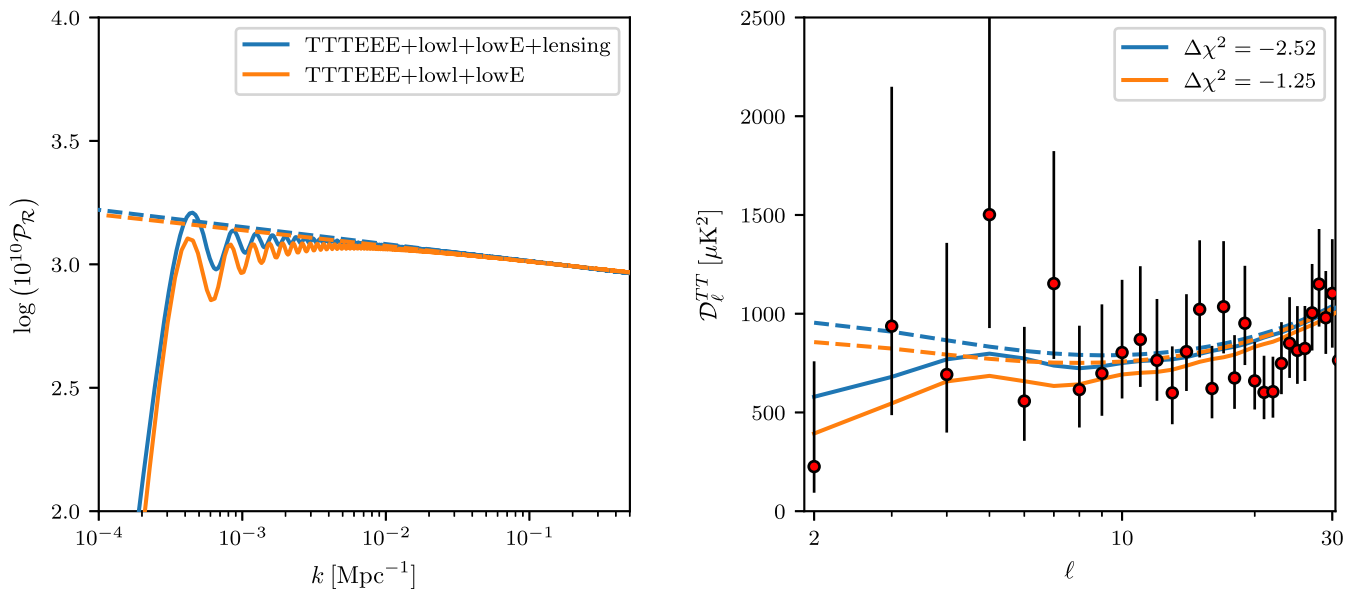


FIG. 3. Primordial power spectra varying the amount of late time curvature. With CMB lensing data, the best-fit cosmology has $\Omega_K = -0.9\%$, while without CMB lensing $\Omega_K = -4.5\%$. Varying the amount of late time to this degree does not affect the location of the cutoff, but does adjust the suppression of power. The inclusion of the full numerical power spectrum in both cases results in an improved fit. Initial conditions are Bunch-Davies and both are chosen to have the “minimum primordial curvature.”

spectrum. Given the degeneracies between cosmological parameters, it is possible that the $\Delta\chi^2$ could be significantly enhanced under a full fitting.

This work will be followed by paper detailing a Bayesian fit [48] for these $K\Lambda$ CDM universes with exact power spectra [44]. It remains to be seen whether the improved $\Delta\chi^2$ will be strong enough to balance the Occam penalty arising from the introduction of an additional constrained primordial parameter.

To see how these results vary as the amount of late-time curvature is altered in Fig. 3, the fit from Fig. 1 is compared with the corresponding fit for the Planck data excluding CMB lensing, which has a significantly higher curvature of $\Omega_K = -4.5\%$ (as opposed to -0.9%). In this case, the location of the suppression of power and the oscillations are barely changed, although as expected [14] the depth of the suppression is greater for the case with more negative curvature.

It should be noted that at the time of writing there is renewed interest in curved cosmologies in light of the controversial work by Di Valentino *et al.* [49] (and also [50]). In these analyses, it is pointed out the Planck CMB primary data are in 2.5σ and 3σ tension with CMB lensing and baryon acoustic oscillation (BAO) data if curvature is included as a free parameter. Such results do not prove that the universe is curved, but arguably weaken the evidence for a flat universe since inconsistent datasets should not be combined. The cause of this tension could be an improbable statistical fluctuation, or could indicate a systematic error in one or more of the datasets. For example, it has been suggested recently that while BAO likelihoods are

curvature agnostic, the compression strategies applied to the observational data do depend on curvature [51], and the default is to assume a flat cosmology for performing this compression. These kind of baked-in flatness assumptions (if present) could bias the curvature constraint provided by BAO. Similarly, the CMB lensing likelihood expands to first order about a fiducial flat cosmology, and a full cross-check expanding about the best-fit $\Omega_K = -4.5\%$ cosmology has not yet been performed.

V. CONCLUSIONS

In this work, the Mukhanov-Sasaki equations and actions for curved cosmologies were derived and discussed. It was found that including an exact numerical calculation for the primordial power spectrum gives a better fit to the data, and that current datasets are capable of distinguishing between alternative definitions of the quantum vacuum. It remains to be seen whether a more complete Bayesian fitting procedure yields compelling evidence for universes with curvature, or the ability to distinguish quantum vacua.

ACKNOWLEDGMENTS

I am indebted to Anthony Lasenby, Mike Hobson, Lukas Hergt, Fruzsina Agocs, Denis Werth, and Maxime Jabarian for their many conversations and participation in the ongoing theoretical and observational research programming stemming from this work. I thank Gonville and Caius College for their continuing support via a Research Fellowship.

- [1] A. A. Starobinskiĭ, Spectrum of relict gravitational radiation and the early state of the universe, *Sov. J. Exp. Theor. Phys. Lett.* **30**, 682 (1979).
- [2] A. H. Guth, Inflationary universe: A possible solution to the horizon and flatness problems, *Phys. Rev. D* **23**, 347 (1981).
- [3] A. D. Linde, A new inflationary universe scenario: A possible solution of the horizon, flatness, homogeneity, isotropy and primordial monopole problems, *Phys. Lett.* **108B**, 389 (1982).
- [4] N. Aghanim *et al.* (Planck Collaboration), Planck 2018 results. VI. Cosmological parameters, [arXiv:1807.06209](https://arxiv.org/abs/1807.06209).
- [5] Y. Akrami *et al.* (Planck Collaboration), Planck 2018 results. X. Constraints on inflation, [arXiv:1807.06211](https://arxiv.org/abs/1807.06211).
- [6] Y. Akrami *et al.* (Planck Collaboration), Planck 2018 results. VII. Isotropy and statistics of the CMB, [arXiv:1906.02552](https://arxiv.org/abs/1906.02552).
- [7] A. G. Riess, S. Casertano, W. Yuan, L. Macri, J. Anderson, J. W. MacKenty, J. B. Bowers, K. I. Clubb, A. V. Filippenko, D. O. Jones, and B. E. Tucker, New parallaxes of galactic cepheids from spatially scanning the Hubble Space Telescope: Implications for the Hubble constant, *Astrophys. J.* **855**, 136 (2018).
- [8] S. Joudaki, C. Blake, C. Heymans, A. Choi, J. Harnois-Deraps, H. Hildebrandt, B. Joachimi, A. Johnson, A. Mead, D. Parkinson, M. Viola, and L. van Waerbeke, CFHTLenS revisited: Assessing concordance with Planck including astrophysical systematics, *Mon. Not. R. Astron. Soc.* **465**, 2033 (2017).
- [9] F. Köhlinger, M. Viola, B. Joachimi, H. Hoekstra, E. van Uitert, H. Hildebrandt, A. Choi, T. Erben, C. Heymans, S. Joudaki, D. Klaes, K. Kuijken, J. Merten, L. Miller, P. Schneider, and E. A. Valentijn, KiDS-450: The tomographic weak lensing power spectrum and constraints on cosmological parameters, *Mon. Not. R. Astron. Soc.* **471**, 4412 (2017).
- [10] H. Hildebrandt *et al.*, KiDS-450: Cosmological parameter constraints from tomographic weak gravitational lensing, *Mon. Not. R. Astron. Soc.* **465**, 1454 (2017).
- [11] T. M. C. Abbott, F. B. Abdalla, A. Alarcon, J. Aleksić, S. Allam, S. Allen, A. Amara, J. Annis, J. Asorey, S. Avila *et al.* Dark energy survey year 1 results: Cosmological constraints from galaxy clustering and weak lensing, *Phys. Rev. D* **98**, 043526 (2018).
- [12] W. Handley and P. Lemos, Quantifying tension: Interpreting the DES evidence ratio, *Phys. Rev. D* **100**, 043504 (2019).
- [13] J.-P. Uzan, U. Kirchner, and G. F. R. Ellis, Wilkinson microwave anisotropy probe data and the curvature of space, *Mon. Not. R. Astron. Soc.* **344**, L65 (2003).
- [14] A. Lasenby and C. Doran, Closed universes, de Sitter space, and inflation, *Phys. Rev. D* **71**, 063502 (2005).
- [15] N. Aghanim *et al.* (Planck Collaboration), Planck 2018 results. VIII. Gravitational lensing, [arXiv:1807.06210](https://arxiv.org/abs/1807.06210).
- [16] S. Alam *et al.*, The clustering of galaxies in the completed SDSS-III baryon oscillation spectroscopic survey: Cosmological analysis of the DR12 galaxy sample, *Mon. Not. R. Astron. Soc.* **470**, 2617 (2017).
- [17] F. Beutler, C. Blake, M. Colless, D. H. Jones, L. Staveley-Smith, L. Campbell, Q. Parker, W. Saunders, and F. Watson, The 6dF galaxy survey: Baryon acoustic oscillations and the local Hubble constant, *Mon. Not. R. Astron. Soc.* **416**, 3017 (2011).
- [18] A. J. Ross, L. Samushia, C. Howlett, W. J. Percival, A. Burden, and M. Manera, The clustering of the SDSS DR7 main Galaxy sample—I. A 4 per cent distance measure at $z = 0.15$, *Mon. Not. R. Astron. Soc.* **449**, 835 (2015).
- [19] W. J. Handley, S. D. Brechet, A. N. Lasenby, and M. P. Hobson, Kinetic initial conditions for inflation, *Phys. Rev. D* **89**, 063505 (2014).
- [20] L. T. Hergt, W. J. Handley, M. P. Hobson, and A. N. Lasenby, Case for kinetically dominated initial conditions for inflation, *Phys. Rev. D* **100**, 023502 (2019).
- [21] E. Ramirez and D. J. Schwarz, Predictions of just-enough inflation, *Phys. Rev. D* **85**, 103516 (2012).
- [22] M. Cicoli, S. Downes, B. Dutta, F. G. Pedro, and A. Westphal, Just enough inflation: power spectrum modifications at large scales, *J. Cosmol. Astropart. Phys.* **12** (2014) 030.
- [23] D. Boyanovsky, H. J. de Vega, and N. G. Sanchez, CMB quadrupole suppression. I. Initial conditions of inflationary perturbations, *Phys. Rev. D* **74**, 123006 (2006).
- [24] D. Boyanovsky, H. J. de Vega, and N. G. Sanchez, CMB quadrupole suppression. II. The early fast roll stage, *Phys. Rev. D* **74**, 123007 (2006).
- [25] V. F. Mukhanov, H. A. Feldman, and R. H. Brandenberger, Theory of cosmological perturbations, *Phys. Rep.* **215**, 203 (1992).
- [26] Z. De-Hai and S. Cheng-Yi, An exact evolution equation of the curvature perturbation for closed universe, *Chin. Phys. Lett.* **21**, 1865 (2004).
- [27] S. Gratton, A. Lewis, and N. Turok, Closed universes from cosmological instantons, *Phys. Rev. D* **65**, 043513 (2002).
- [28] B. Ratra, Inflation in a closed universe, *Phys. Rev. D* **96**, 103534 (2017).
- [29] B. Bonga, B. Gupta, and N. Yokomizo, Inflation in the closed FLRW model and the CMB, *J. Cosmol. Astropart. Phys.* **10** (2016) 031.
- [30] B. Bonga, B. Gupta, and N. Yokomizo, Tensor perturbations during inflation in a spatially closed Universe, *J. Cosmol. Astropart. Phys.* **05** (2017) 021.
- [31] S. Akama and T. Kobayashi, General theory of cosmological perturbations in open and closed universes from the Horndeski action, *Phys. Rev. D* **99**, 043522 (2019).
- [32] J. Ooba, B. Ratra, and N. Sugiyama, Planck 2015 constraints on the non-flat Λ CDM inflation model, *Astrophys. J.* **864**, 80 (2018).
- [33] Maplesoft, a division of Waterloo Maple Inc., Waterloo, Ontario, Maple 2017, 2017.
- [34] M. B. Monagan, K. O. Geddes, K. M. Heal, G. Labahn, S. M. Vorkoetter, J. McCarron, and P. DeMarco, *Maple 10 Programming Guide* (Maplesoft, Waterloo ON, Canada, 2005).
- [35] J. Lesgourgues and T. Tram, Fast and accurate CMB computations in non-flat FLRW universes, *J. Cosmol. Astropart. Phys.* **09** (2014) 032.
- [36] D. Baumann, TASI lectures on inflation, [arXiv:0907.5424](https://arxiv.org/abs/0907.5424).
- [37] R. Arnowitt, S. Deser, and C. W. Misner, Republication of: The dynamics of general relativity, *Gen. Relativ. Gravit.* **40**, 1997 (2008).

- [38] T. Prokopec and J. Weenink, Uniqueness of the gauge invariant action for cosmological perturbations, *J. Cosmol. Astropart. Phys.* **12** (2012) 031.
- [39] W.J. Handley, A.N. Lasenby, and M.P. Hobson, Novel quantum initial conditions for inflation, *Phys. Rev. D* **94**, 024041 (2016).
- [40] W.J. Handley, A.N. Lasenby, and M.P. Hobson, The Runge-Kutta-Wentzel-Kramers-Brillouin method, [arXiv:1612.02288](https://arxiv.org/abs/1612.02288).
- [41] W.I.J. Haddadin and W.J. Handley, Rapid numerical solutions for the Mukhanov-Sasaki equation, [arXiv:1809.11095](https://arxiv.org/abs/1809.11095).
- [42] F.J. Agocs, W.J. Handley, A.N. Lasenby, and M.P. Hobson, An efficient method for solving highly oscillatory ordinary differential equations with applications to physical systems, [arXiv:1906.01421](https://arxiv.org/abs/1906.01421).
- [43] J. Bamber and W. Handley, Beyond the Runge-Kutta-Wentzel-Kramers-Brillouin method, [arXiv:1907.11638](https://arxiv.org/abs/1907.11638).
- [44] L.T. Hergt, W.J. Handley, M.P. Hobson, and A.N. Lasenby, Constraining the curved kinetically dominated Universe (to be published).
- [45] P. Labraña, Emergent Universe scenario and the low CMB multipoles, *J. Phys. Conf. Ser.* **720**, 012016 (2016).
- [46] G.F.R. Ellis and R. Maartens, The emergent universe: Inflationary cosmology with no singularity, *Classical Quantum Gravity* **21**, 223 (2004).
- [47] D. Blas, J. Lesgourgues, and T. Tram, The cosmic linear anisotropy solving system (CLASS). Part II: Approximation schemes, *J. Cosmol. Astropart. Phys.* **07** (2011) 034.
- [48] L.T. Hergt, W.J. Handley, M.P. Hobson, and A.N. Lasenby, Constraining the kinetically dominated universe, *Phys. Rev. D* **100**, 023501 (2019).
- [49] E. Di Valentino, A. Melchiorri, and J. Silk, Planck evidence for a closed Universe and a possible crisis for cosmology, *Nat. Astron.* (2019).
- [50] W. Handley, Curvature tension: evidence for a closed universe, [arXiv:1908.09139](https://arxiv.org/abs/1908.09139).
- [51] M. O’Dwyer, S. Anselmi, G.D. Starkman, P.-S. Corasaniti, R. K. Sheth, and I. Zehavi, Linear point and sound horizon as purely geometric standard rulers, [arXiv:1910.10698](https://arxiv.org/abs/1910.10698).